ARCHIVES
of
FOUNDRY ENGINEERING

ISSN (2299-2944)
Volume 2023
Issue 4/2023

5 – 13

10.24425/afe.2023.146673

1/4

Published quarterly as the organ of the Foundry Commission of the Polish Academy of Sciences

Evaluation of the Phases Present in the Zinc Coating Obtained on the Ductile Cast Iron Substrate in the Bath with the Addition of Ti

K.Z. Bracka-Kęsek*, A. Szczęsny, D. Kopyciński, E. Guzik
AGH University of Science and Technology, Department of Foundry Engineering,
Al. Mickiewicza 30, 30-059 Kraków, Poland
*Corresponding author. E-mail address: bracka@agh.edu.pl

Received 30.03.2016; accepted in revised form 14.07.2023; available online 07.11.2023

Abstract

This paper presents the effect of the addition of Ti to the zinc bath. Hot-Dip Galvanizing was carried out on a machined ductile cast iron substrate. The process was carried out at 550°C. Experimental baths A, B and C contained 0.01%, 0.05% and 0.1%Ti, respectively. Metallographic samples were prepared to reveal the microstructure of the coatings. Thickness measurements of the obtained coatings were carried out, and graphs of the approximate crystallization kinetics of the zinc coating were prepared. High-temperature galvanization carried out on the treated surface led to the release of graphite beads from the metal matrix and their diffusion into the coating. This phenomenon can have an adverse effect on the continuity of the coating and its adhesion to the substrate. Crystallization of the δ phase was observed in the coating, and at longer immersion times – a mixture of two-phase δ1 and η phases. With increasing Ti content in the bath, a deterioration in the casting properties of the bath was observed.

Keywords: Hot-dip galvanizing, Fe-Zn-Ti, Ti addition, Cast iron

1. Introduction

The process of hot dip galvanizing is a well-known and widely used way to protect steel products from corrosion. Its low cost, high availability and long corrosion protection time allows for wide and mass use of this technique. Obtaining zinc coatings allows to extend the service life of products and consequently to reduce operating costs. [1-4]

The final microstructure and properties of the coatings are influenced by physical factors such as bath temperature (phase formation in the high-temperature process takes place bypassing the zeta phase), substrate surface (on a rough substrate thicker layers grow) or bath incubation time of the sample, and chemical factors, such as the chemical composition of the zinc bath (the alloying additives used affect film formation), bath cleanliness, the chemical composition of the galvanising substrate (thicker films grow on a high-silicon substrate and spheroidal graphite precipitates can cause discontinuities in the coatings) and the flux used in the process. [5, 6] The high-temperature process is usually carried out above the temperature range where the 'zinc erosion' of iron is most intense.

2. Analysis of the phase equilibrium system of Fe-Zn alloys

In order to properly analyze a zinc coating formed on an Fe-C alloy substrate, it is necessary to know and understand the Fe-Zn

phase equilibrium system in detail. This allows us to accurately interpret the crystallization kinetics of the zinc coating depending on the chemical composition and the temperature of the galvanizing process. The most important issue is the equilibrium states between the liquid phase and the crystallizing intermetallic phases. Fig. 1 shows the zinc-rich part of the Fe-Zn phase equilibrium system. It is a system that takes into account changes that have progressed with subsequent analyses and discoveries in this area.

Delta phase: 530°C-672°C, zeta phase 419.4°C-530°C. These are the phases found in the samples studied. However, it should be taken into account that the phase equilibrium system does not assume alloying additives. The addition of titanium to the bath can affect the change in the temperatures of transformations occurring due to diffusion of atoms. Tab. 1. shows the given names of the phases along with their sum formulas and crystal lattice structure.

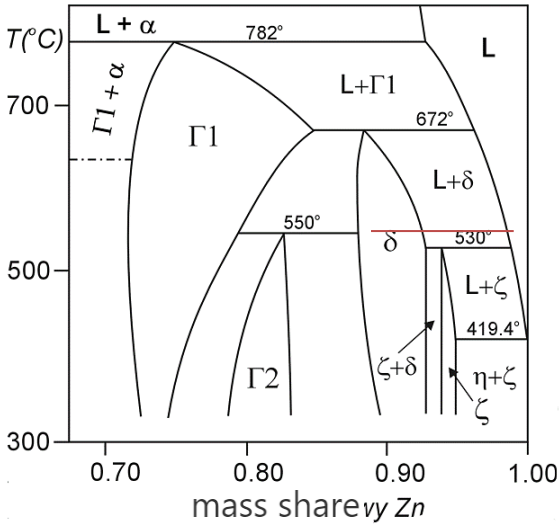

Fig. 1. Zn-rich part of the phase equilibrium system of Fe-Zn alloys [9-11]

As a result of the process, a coating is formed in which the zinc content increases from the substrate boundary to the coating surface. The various intermetallic phases are characterized by different morphology, structure, and consequently also by strength and corrosion properties. [7]

Fig. 2. shows the basic intermetallic phases present in zinc coating on steel substrates and on ductile cast iron substrates in Fig. 3. We can distinguish 4 Fe-Zn intermetallic phases with different Fe and Zn contents. They are formed by the diffusion of zinc atoms toward the substrate and iron atoms toward the bath. The intermetallic phases in the classical galvanizing process, which is carried out at a temperature of about 450°C for steel products, are formed sequentially from the substrate: as the first zeta phase with the highest Zn content, followed by the delta phase with an iron content of 7-11.5 wt. %, and finally the gamma phase 17-19 wt. % Fe. [8] The thickness of the η phase, which contains almost zinc itself, has a significant effect on Zn consumption in the dip galvanizing process.

The process was carried out at 550°C, which also allowed the delta phase in the alloy layer first.

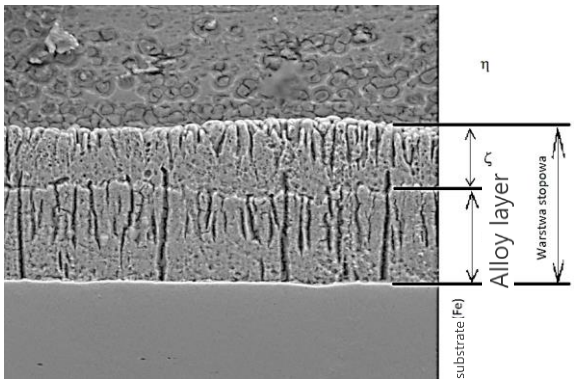

Fig. 2. Phases present in the zinc coating obtained on a steel substrate during the galvanizing process at 450°C

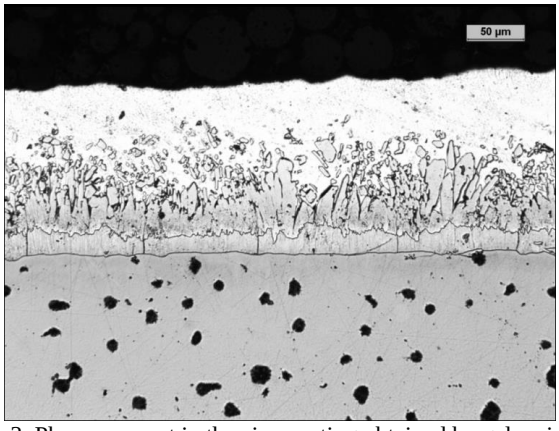

Fig. 3. Phases present in the zinc coating obtained by galvanizing on a ductile cast iron substrate at 450°C in the 600s time immersion [3]

Fig. 4. shows the effect of the temperature of conducting the galvanizing process on iron loss in galvanizing baths. Conducting the galvanizing process in the temperature range from about 470°C to about 525°C can result in very rapid destruction of the galvanizing bath. This can be considered a technological limitation, as the process is safest conducted in non-reactive crucibles with baths that are limited in size, so there would be a limitation in the size of the products being galvanized or the need for non-reactive coated baths, which directly increases the cost of the process. In the study, the molten bath was in a ceramic crucible, so this was not relevant, but given the industrial reality, one must be aware of such phenomena.

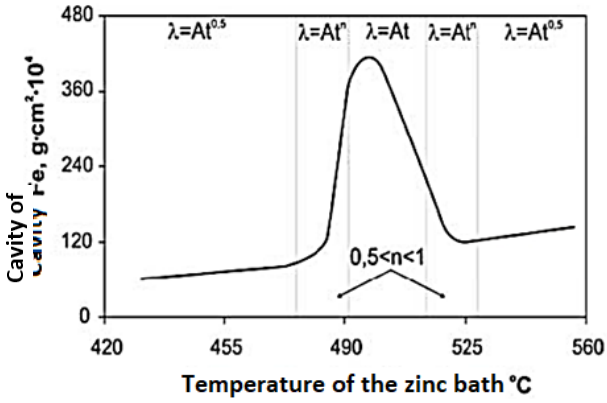

Fig. 4. Effect of zinc bath temperature on coating growth kinetics and iron loss due to "zinc erosion" [4]

Tab. 1. summarizes the ranges of Zn concentrations in intermetallic phases occurring in the Fe-Zn system as determined experimentally or determined theoretically over several decades of research by researchers around the world.

Table 1.
Zn concentration ranges in Fe-Zn intermetallic phases recorded in the literature by the authors [9-35]

Phase	Γ1 - Fe_3Zn_{10}	Γ2 - Fe_5Zn_{21}	δ - $FeZn_7$ δ - $FeZn_{10}$	ζ - $Fe\text{-}Zn_{13}$
Authors	Budowa krystaliczna			
	Regular spatially centered	Regular flat-centered	Heksagonal	Single slant
	wt. % Zn			
Hansen	0.7199 ÷ 0.7903		0.8868 ÷ 0.9247	0.9378 ÷ 0.9404
Truesdale	0.7302 ÷ 0.8004		0.8850 ÷ 0.9370	-
Schramm				0.9378 ÷ 0.9396
Cigan	0.7320 ÷ 0.8150		0.8957 ÷ 0.9352	0.9465 ÷ 0.9483
Bühler	0.6669 ÷ 0.8059		δ_C 0.8832÷0.8921 δ_P 0.9133÷0.9238	0.9326 ÷ 0.9422
Bastin	-	0.7921 ÷ 0.8376	-	-
Onishi	-	-	-	0.9177
Short, Mackowiak	0.6352 ÷ 0.6764	0.7790 ÷ 0.7821	0.8520 ÷ 0.8913	0.8939 ÷ 0.8957
Gellings	-	-	0.8824 ÷ 0.9265	0.9378 ÷ 0.9422
Kubaschewski	0.7227 ÷ 0.8421	0.7784 ÷ 0.8331	0.8779 ÷ 0.9307	~0.9396
Burton, Perrot	0.7200 ÷ 0.8500 L+α-Fe→0.7500	0.8100 ÷0. 8300 -	0.8850 ÷ 0.9300 L+Γ→88,70	0.9400 ÷ 0.9480 L+δ→0.9400
Marder	0.7200 ÷ 0.7650	0.8050 ÷0.8300	0.8850 ÷ 0.9300	0.9400 ÷ 0.9500
Su	L+α(Fe)→0.7618	-	L+Γ→ 0.8859	L+ζ→ 0.9383

3. Preparation of the experiment

Hot-Dip Galvanizing is a process that consists of several steps. Despite the alloying additives used, the preparatory process for immersion was carried out as in classical galvanizing of steel (except for the bath temperature). The raw surface of the iron specimens was sanded while cutting the samples with an angle grinder. Ductile iron graded according to EN/GJS/500-7 was used as the substrate material. Bead graphite separations have a significant effect on the continuity of the obtained coatings on the machined surface. The arithmetic mean deviation of the roughness profile Ra=1.22μm and the maximum height of the roughness profile Rz=8.43μm.

Figure 5 shows a schematic of the specimen along with its dimensions. The specimens were 5mm thick.

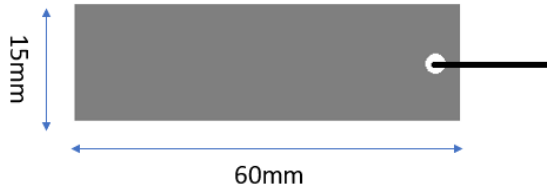

Fig. 5. Diagram of a cast iron specimen immobilised on a steel wire

The samples prepared in this way should be subjected to preparatory treatment consisting of several steps:

- degreasing the samples with anhydrous ethanol (ETANOL 99.8%),

- rinsing under a stream of running water,
- drying in a stream of warm air blowing in a laboratory dryer,
- digestion of samples in 16%HCl,
- rinsing under a stream of running water the residual acid along with the etching products from the surface of the samples,
- re-drying the samples,
- treatment of the samples at 70°C in a 35 percent aqueous solution of a ZnCl2/NH4Cl salt mixture (up to 5 minutes) to activate the substrate surface before the basic immersion galvanization process,
- final drying of the samples,
- immersion galvanization in a zinc bath at 550°C for 60, 180 and 360s,
- cooling of the samples in water to quickly stop crystallization and transformation of the resulting coating.

The zinc baths were prepared using a 50 Hz PET electric crucible resistance furnace in a ceramic crucible to avoid reacting the bath with the furnace lining. Fig. 7. shows the bath melting station. The process was carried out at 550°C ± 5°C. This temperature is marked on the phase equilibrium system in Fig. 1. The temperature during the process was measured using a thermocouple, which was connected to the automatic control system of the digital measurement of the furnace controller to automatically stabilize and regulate the temperature.

The process diagram is shown in Fig. 6.

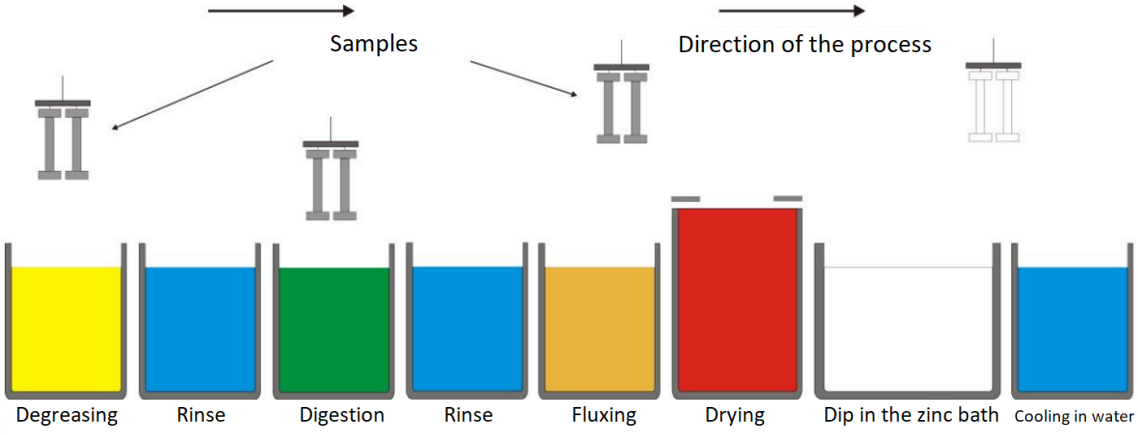

Fig. 6. Steps in conducting the dip galvanizing process

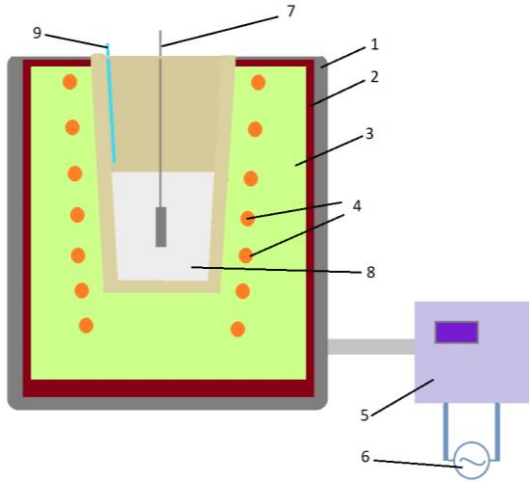

Fig. 7. Test stand prepared for immersion galvanizing of ductile cast iron. Figure description: 1 - zinc bath, 2 - crucible, 3 - steel rod with suspended sample, 4 - resistance heating elements, 5 - chamotte lining, 6 - insulating material, 7 - steel housing, 8 - automatic furnace temperature control system, 9 - source of electric voltage

3.1. Composition of zinc baths

The composition of the zinc bath is one of the most important parameters for conducting the galvanizing process. Through the use of alloying additives, we create the possibility of influencing coating properties such as corrosion resistance, alloy layer thickness, as well as the appearance of the outer surface of the coating. In this study, an alloying additive in the form of titanium was used at different concentrations. Baths were prepared based on a metal charge prepared from pure components. The assumed chemical compositions are shown in Table 2.

Table 2.
Chemical composition of zinc baths

Bath	Addition Ti
0	0 wt.%
A	0,01 wt.%
B	0,05 wt.%
C	0,1 wt.%

At the stage of conducting the smelting, difficulties in running the process were observed. As the Ti content in the zinc bath increased, the metal mirror oxidized faster, and the resulting coating made it difficult to run the process properly.

In addition, the effect of the Ti additive on the leaminess and surface tension of the bath was noted. At higher Ti contents, when pulling the sample out of the bath, the excess metal had increasing difficulty to flow off. This resulted in the formation of droplets at the end of the sample and, ultimately, the obtaining of thicker zinc layers.

4. Metallographic analysis of the microstructure of zinc coatings on ductile cast iron surfaces

For metallographic analysis, it is necessary to reveal the surface of the deposit. Samples were cut perpendicular to the galvanizing surface. The metallographic deposit was then ground on a Roto-Pol laboratory grinder using magnetic abrasive discs with gradations ranging from 80ppm to 600ppm. The surface was then sanded on a polishing cloth in the presence of a lubricant and diamond slurry. The samples prepared in this way were etched with Villel's reagent and then rinsed in ethanol. Samples with higher Ti content required etching for a longer time to reveal the interfacial boundaries. Metallographic specimens were observed using a Leica optical microscope equipped with a Leica Q-Win automated image analyzer. Figs. 8-11 show the microstructures obtained in zinc baths with different Ti additions after incubation times of 60, 180 and 360 seconds. The blue color indicates the delta phase layer, while the red color indicates the mixture of phases $\delta 1+ \eta$.

In addition, Figure 12 shows the SEM microstructure with marked points for chemical composition analysis. The study was performed with a repeated, deeper etching with Villel reagent. Observations were carried out using a JEOL 500LV brand scanning electron microscope equipped with an X-ray microanalysis attachment.

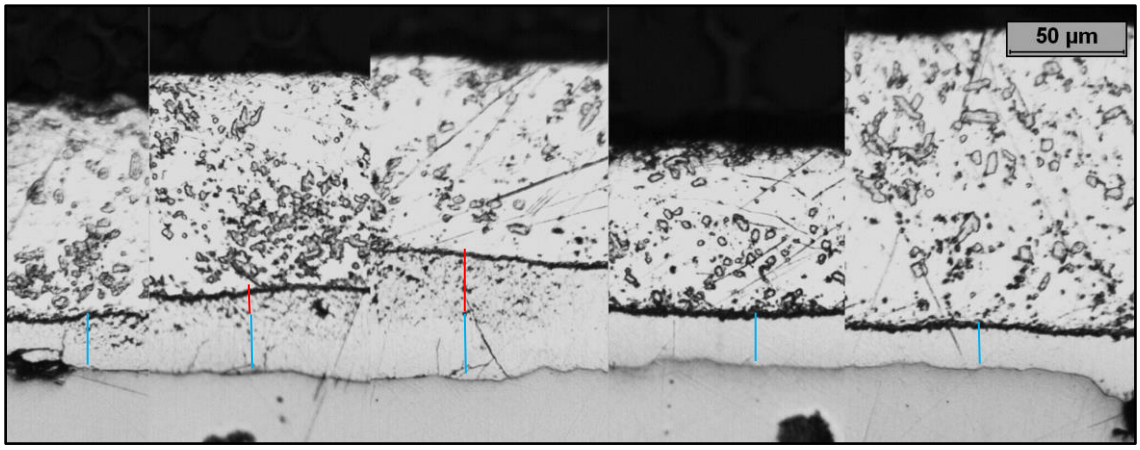

Fig. 8. Microstructure of coatings obtained at times from left: 60, 180, 360, 600, 900s in bath 0

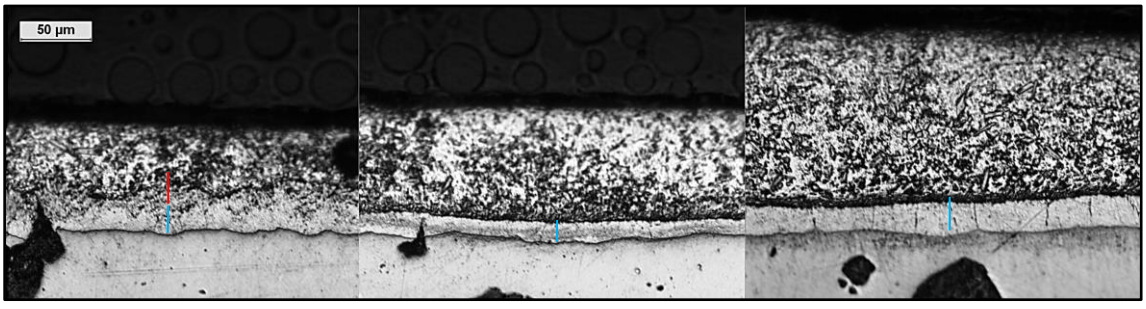

Fig. 9. Microstructure of coatings obtained at times from left: 60, 180, 360s in bath A

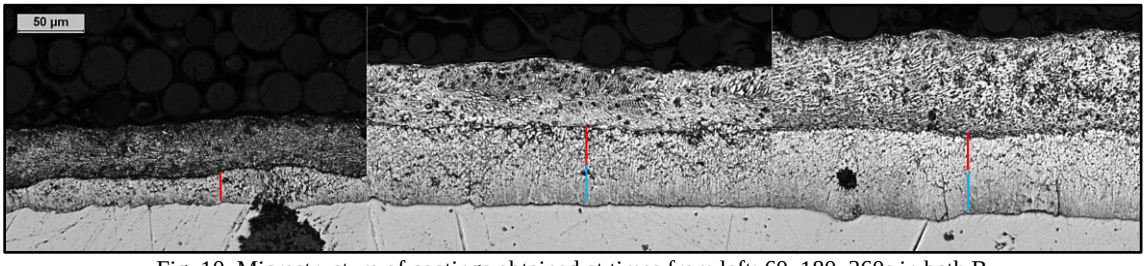

Fig. 10. Microstructure of coatings obtained at times from left: 60, 180, 360s in bath B

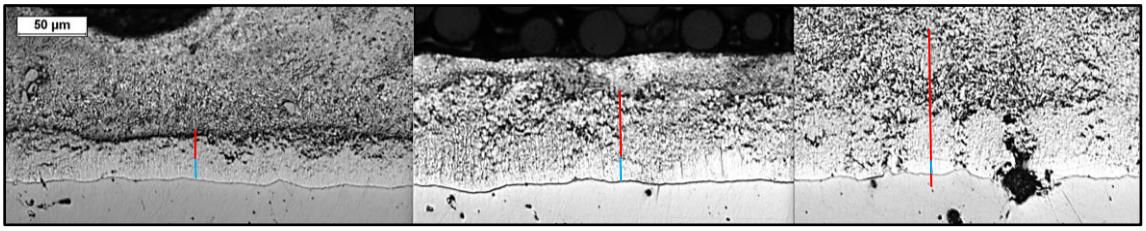

Fig. 11. Microstructure of coatings obtained at times from left: 60, 180, 360s in bath C

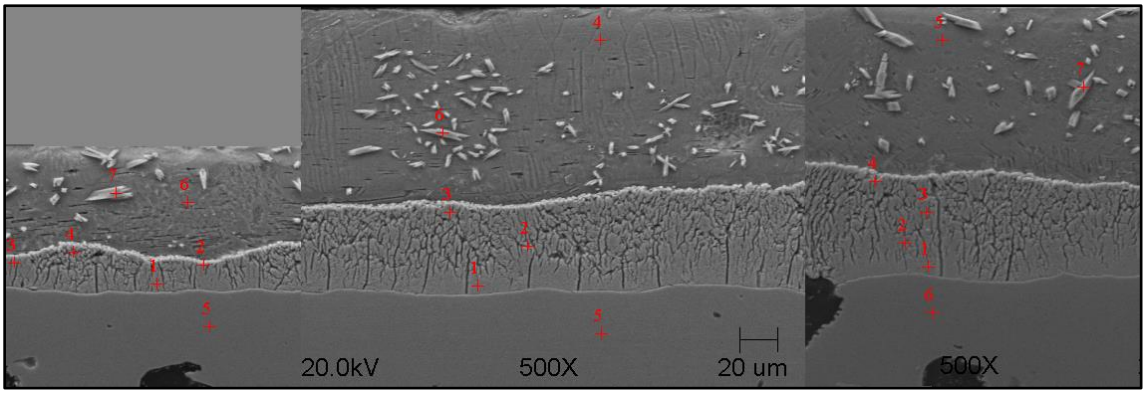

Fig. 12. Microstructure SEM of coatings obtained at times from left: 60, 180, 360s in bath A

Table 3.
Results of spot chemical composition analysis of coatings obtained in bath A

	60s				180s				360s			
	Si	Ti	Fe	Zn	Si	Ti	Fe	Zn	Si	Ti	Fe	Zn
1	0.469	0.059	10.66	88.811	0.352	0.137	12.224	87.287	0.342	0.102	10.932	88.624
2	0.148	0.026	4.899	94.927	0.139	0.118	8.637	91.105	0.234	0.136	9.049	90.581
3	0.118	0.038	6.377	93.467	0.237	0.058	6.728	92.977	0.123	0.079	7.382	92.416
4	0.269	0.129	7.342	92.26	0.103	0.194	0.175	99.528	0.204	0.051	6.318	93.427
5	1.25	0	98.75	0	1.265	0.084	98.507	0.145	0.059	0.024	0.162	99.755
6	0.145	0.042	0.255	99.558	0.06	0.121	0.625	99.194	1.25	0	98.75	0
7	0.127	0.021	1.503	98.349					0.361	0.109	5.573	93.957

Ti was observed in the alloy layer. It is worth noting that the Ti content in the alloy layer is significantly higher than in the zinc bath. The precipitates dispersed in the outer layer of the coating, are also characterised by a Ti content higher than in the bath.

The microstructure of the sample made in bath A after holding the sample in the 60s bath is very irregular, it is difficult to distinguish the interfacial boundary, it is very extensive.

Increasing the incubation time to 360s resulted in a much more regular structure, it is compact, without extensive hard zinc precipitates, while maintaining a very small thickness of the alloy layer, but also the overall layer formed during the galvanization process.

The resulting coatings have different structures. As the incubation time of the sample in the bath increases, the thickness of the resulting coatings increases. The thickness of the coatings has been measured and is shown in the Tab. 3, distinguishing the alloy layer and the various intermetallic phases.

Table 3.
Thickness of the obtained coatings in micrometers

	Immersion Time	0	A	B	C
Alloy layer	60s	25	15-25	20	25-30
	180s	40	15	55	60-75
	360s	50	20	62	>200
δ Phase	60s	25	15	20	12
	180s	25	15	20-25	12-25
	360s	25	20	25-30	12
Biphases mixture δ1 and η	60s	x	0-5	x	12-25
	180s	15	x	30	25-30
	360s	25	x	30-35	>200

The thickness of the alloy layer increases with both the increase of Ti in the zinc bath and the incubation time of the sample in the zinc bath. In Figs. 13-15, the thicknesses of the sub-layers of the alloy layer are illustrated in graphs. It consists of a delta phase layer from the substrate and a further layer of hard zinc. We can

definitely consider the C bath as the most reactive one, since the alloy layer grows much faster and to an extreme when the incubation time is increased to 360s.

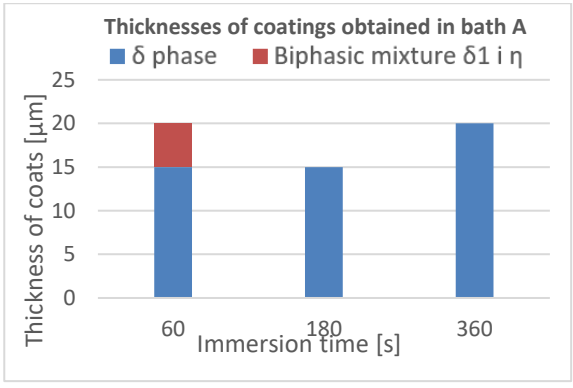

Fig. 13. Plot of coating thickness versus incubation time of the sample in the bath from left: 60, 180, 360s

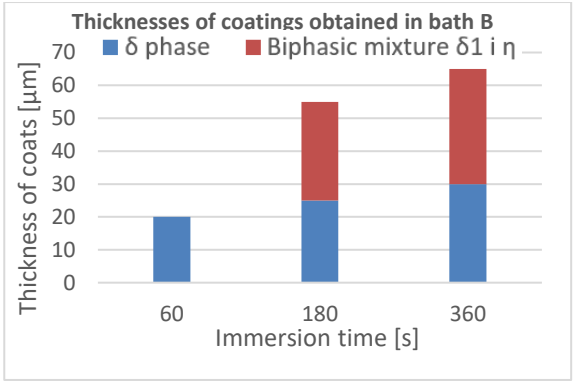

Fig. 14. Plot of coating thickness versus incubation time of the sample in the bath from left: 60, 180, 360s

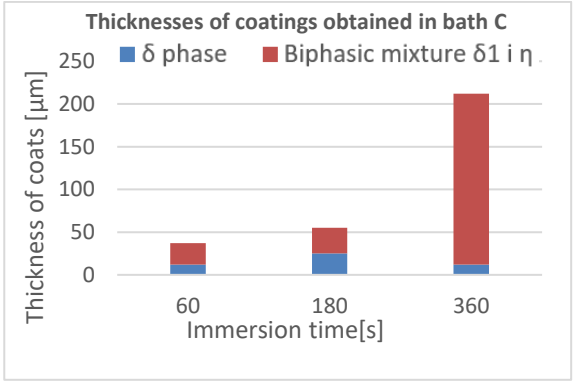

Fig. 15. Plot of coating thickness versus incubation time of the sample in the bath from left: 60, 180, 360s

A stabilization of the thickness of the delta layer was observed regardless of the incubation time. Differences in the thickness of this phase between successive samples were about 5 micrometers.

The process was carried out at 550°C, so it would not be probable to first form the zeta phase, as it occurs during immersion metallization at 450°C would not be likely.

The delta phase increases first at this temperature, and when the incubation time is extended, diffusion of atoms takes place due to the concentration difference. [35] Subsequently, a distinct sublayer composed of δ1+ η phases is formed, as confirmed by the authors in the publication. [36]

In addition, during longer incubation times at this galvanizing temperature, the probability of the formation of hard zinc precipitates increases, which is a very unfavorable effect due to bath wear and waste formation.

On the basis of the measurement of coating thickness, we can approximate the kinetics of the growth of these phases over time. In Figs. 16-18, the trend of growth and stabilization of the phases can be seen.

It is also worth noting the type of graphite precipitates in the galvanised iron. The presence of these precipitates can cause discontinuities in the resulting coating, but surface treatments can be carried out to remove the graphite from the surface so that the diffusion of Fe atoms from the substrate and Zn atoms from the bath is not impaired. [37]

Furthermore, the immersion galvanising process is not indifferent to the substrate matrix. Immersion in the zinc bath leads to overheating of the sample and can lead to interfacial transformations in the substrate. [38] On the one hand, a phenomenon of this kind can be regarded as a threat to the loss of the beneficial properties of the galvanised component. However, the potential of combining the hot-dip galvanising process with the heat treatment of the substrate can be sought in a solution of this type.

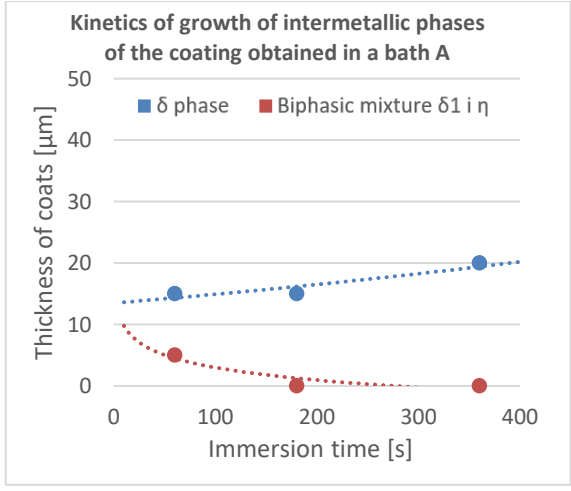

Fig. 16. Graph of growth kinetics of intermetallic phases of the coating obtained in bath A

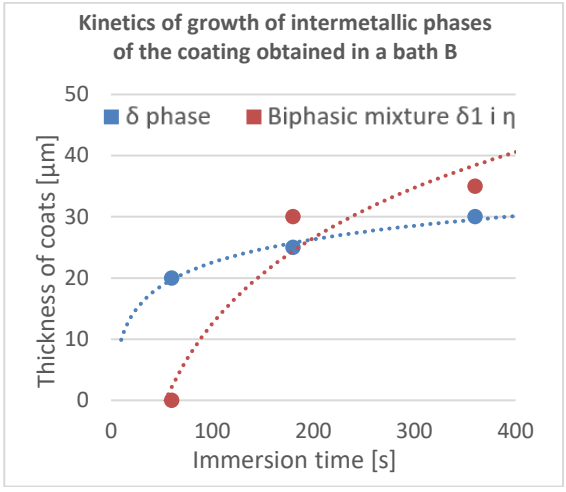

Fig. 17. Graph of growth kinetics of intermetallic phases of the coating obtained in bath B

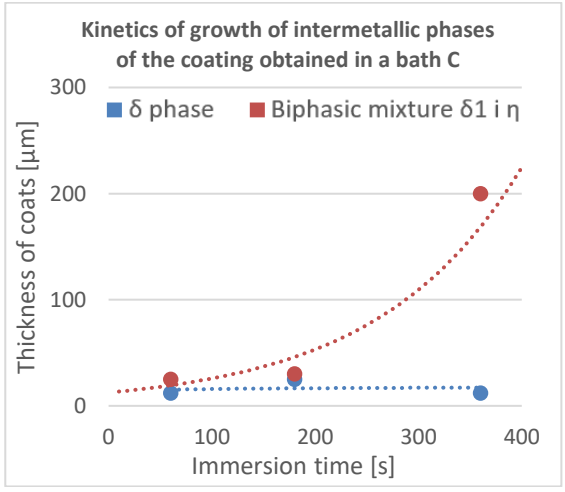

Fig. 18. Graph of growth kinetics of intermetallic phases of the coating obtained in bath C

5. Conclusions

1. The decrease in the funneling and surface tension of the metal with an increase in Ti in the zinc bath results in the formation of a thick layer of the η phase containing trace amounts of Fe. This is definitely an unfavorable effect, as it results in significantly higher wear of the bath in the galvanizing process.
2. Conducting the process at 550°C and using Ti additive to the bath made it possible to obtain thinner alloy layers.
3. The addition of Ti to the zinc bath in the amount of 0.01% results in the inhibition of the growth of the sub-layer consisting of a mixture of delta and eta phases, regardless of the time the sample is kept in the zinc bath.
4. Coatings obtained in baths B and C after extending the time of holding in the bath to 360 significantly thicker than in smelting A.
5. Increasing the incubation time to 6 minutes for ductile iron leads to more intense dissolution of the substrate. The graphite separations thus released can cause discontinuity in the zinc coatings obtained.

References

[1] Kopyciński, D., Guzik, E. & Woźnica, H. (2006). The gradient structure zinc coating shaping at the surface of ductile cast iron. *Archives of Foundry*. 6(22), 278-285.

[2] Kania, H. & Liberski, P. (2012) Synergistic influence of Al, Ni, Bi and Sn addition to a zinc bath upon growth kinetics and the structure of coatings. *Materials Science and Engineering.* 35, 1-10. DOI: 10.1088/1757-899X/35/1/012004.

[3] Kopyciński, D., Guzik, E. & Szczęsny, A. (2014). The effect of the number of eutectic grains on coating growth during hot dip galvanising of ductile iron castings. *Archives of Foundry Engineering*. 14(1), 67-70. ISSN (1897-3310).

[4] Kania, H. & Liberski, P. (2014). The structure and growth kinetics of zinc coatings on link chains produced of the 23MnNiCrMo5-2 steel. *Solid State Phenomena*. 212, 145-150. DOI:10.4028/www.scientific.net/SSP.212.145.

[5] Kopyciński, D., Guzik, E., Szczęsny, A. & Siekaniec, D. (2015). Growth kinetics of the protective coating during high- and low- temperature process of hot dip galvanizing of ductile iron castings. *Archives of Foundry Engineering*. 15(spec.2), 47-50. ISSN (1897-3310). (in Polish).

[6] Kopyciński, D. (2015). Sequence of formation of intermetallic phases in a zinc coating. *Inżynieria Materiałowa*. 5(207), 251-255 DOI 10.15199/28.2015.5.10. (in Polish).

[7] Di Cocco, V. (2012). Sn and Ti influences on intermetallic phases damage in hot dip galvanizing. *Frattura ed Integrità Strutturale.* 22, 31-38. DOI: 10.3221/IGF-ESIS.22.05.

[8] Kania, H. & Liberski, P. (2008). High-temperature galvanizing. *Ochrona przed korozją*. 10, 370-376. (in Polish).

[9] Kubaschewski O. (1982). *Iron – Binary phase diagrams.* Berlin, Springer-Verlag.

[10] Massalski, T.B. (1990). *Binary alloy phase diagrams*. ASM International.

[11] Burton, P.B., Perrot, P. (1993). *Phase diagram of binary iron alloys*. American Society for Metals, Metals Park, OH, 1993, 459-466.

[12] Mackowiak, J. & Short, N.R. (1979). Metallurgy of galvanized coating. *International Metals Reviews*, 1, 1-19.

[13] Schubert, P. & Schultz, W.D. (2001). Was sind „reactive" Stähle – zum Einfluss von Wasserstoff in Baustählen auf die Schichtbildung beim Feuerverzinken. *Metall.* 55(12), 743-748.

[14] Schramm, J. (1936). Das System Eisen-Zink. *Zeitschrift für Metallkunde*, 28, 203-207.

[15] Schramm, J. (1937). Über eine neue Phase im System Eisen – Zink. *Zeitschrift für Metallkunde*. 29, 222-225.

[16] Scheil, E. & Wurst, H. (1937). Über die Reactionen des Eisens mit flüssigem Zink. *Zeitchrift für Metallkunde*, 29, 225-228.

[17] Schramm, J. (1938). Röntgenographische Unterschung der Phasen und Phasen-granzen in den System des ZInks mit Eisen, Kobalt und Nickel. *Zeitschrift für Metallkunde*. 30, 122-130.

[18] Schramm J. (1938). Über die Wärmetönungen der Dreiphasenumsetzungen in den System des Zinks mit Nickel, Kobalt, Eisen und Mangan. *Zeitschrift für Metallkunde*. 30, 131-134.
[19] Ghoniem, M.A. & Löhberg, K. (1972). Über die bei der Feuerverzinkung entstehenden δ_{1p} und δ_{1k} Schichten. *Metall*. 26, 1026-1030.
[20] Bastin, G.F., Loo, F.J.J. & Rieck, G.D. (1974). A new compound in the iron zinc system. *Zeitschrift für Metallkunde*. 65, 656-660.
[21] Bastin, G. F., Loo, F.J.J. & Rieck, G.D. (1976). On the texture in the δ (Fe-Zn) layer formed during hot dip galvanizing. *Zeitschrift für Metallkunde*. 67, 694-698.
[22] Bastin, G.F., Loo, F.J.J. & Rieck, G. D. (1977). On the δ-phase in the Fe-Zn system. *Zeitschrift für Metallkunde*. 68, 359-361.
[23] Gelliings. P.J., Bree. E.W. & Gierman, G. (1979). Synthesis and characterization of homogoneous intermetallic Fe-Zn coumpounds (part I, the δ_1 phase). *Zeitschrift für Metallkunde*. 70, 312-314,
[24] Gelliings, P.J., Bree, E.W. & Gierman, G. (1979). Synthesis and characterization of homogoneous intermetallic Fe-Zn coumpounds (part II: the ζ phase). *Zeitschrift für Metallkunde*. 70, 315-317.
[25] Gelliings, P.J., Gierman, G., Koster, D. & Kuit, J. (1980). Synthesis and characterization of homogoneous intermetallic Fe-Zn coumpounds (part III: Phase diagram). *Zeitschrift für Metallkunde*. 71, 70-75.
[26] Gelliings, P.J., Koster, D., Kuit, J. & Fransen, T. (1980). Synthesis and characterization of homogoneous intermetallic Fe-Zn coumpounds (part IV: thermodynamic properties). Zeitschrift für Metallkunde. 71, 150-154.
[27] Bohran-Tavakoli, A. (1984). Formation and growth of the δ1 phase in the Fe-Zn system. Part II. *Zeitschrift für Metallkunde*. 75, 350-355.
[28] Bohran-Tavakoli, A. (1984). On the formation and growth of the δ1 phase in the Fe-Zn system. Part II. *Zeitschrift für Metallkunde*. 75, 436-439.
[29] Grant, R.G., Cook, P.S. & Cook, D.C. (1995). Preparation and chemical analysys of high purity iron-zinc alloys. *Journal Mater. Research*. 10, 2454-2462.
[30] Liu, Z.T., Boisson, M. & Uwakweh, O.N.C. (1996). Kinetics of phase evolution of Zn-Fe intermetallics. *Metallurgical and Materials Transactions*. 27 A, 2904-2910.
[31] Bastin, G.F. & Loo, F.J. (1978). On the texture in the ζ(Fe-Zn) layer formed during hot dip galvanizing system. *Zeitschrift für Metallkunde*. 69, 540-545.
[32] Hong, M. N. & Saka, H. (1997). Transmition electron microscopy of the iron-zinc δ1 intermetallic phase. *Scripta Materialia*. 36, 1423-1426.
[33] Hong, M.N. & Saka, H. (1997). Plasticity and grain boundry structure of the δ_{1p} and δ_{1k} intermetallic phase in the Fe-Zn system. *Acta Metallurgica*. 45, 4225-4230.
[34] Reumont, G., Perrot, P., Fiorani, J.M. & Hertz, J. (2000). Thermodynamic evaluation of the Fe-Zn system. *Journal of Phase Equilibria*. 21, 371-378.
[35] Mita, K., Ikeda, T., Maeda, M. (2000). Phase diagram study of Fe-Zn intermetallics. *Journal of Phase Equilibria*. 23, 1808-1815.
[36] Su, X., Tang, N.Y. & Toguri, J.M. (2001). Thermodynamic evaluation of the Fe-Zn system. *Journal of Alloys and Compounds*. 325, 129-136.
[37] Jędrzejczyk, D. & Hajduga, M. (2011). Effect of the surface oxidation on the hot-dip zinc galvanizing of cast iron. *Archives of Metallurgy and Materials*. 56(3), 839-849. https://doi.org/10.2478/v10172-011-0093-x.
[38] Jędrzejczyk. D. (2010). The influence of high-temperature treatment of cast iron on the structure of the surface layer formed as a result of hot-dip galvanizing. *Ochrona przed Korozją*. 2, 46-48.